Front. Earth Sci. 2018, 12(3): 555–568
https://doi.org/10.1007/s11707-018-0686-z

RESEARCH ARTICLE

Structural characteristics and implication on tectonic evolution of the Daerbute strike-slip fault in West Junggar area, NW China

Kongyou WU (✉)[1,2], Yangwen PEI (✉)[1,3], Tianran LI[1], Xulong WANG[4], Yin LIU[1], Bo LIU[1], Chao MA[1], Mei HONG[1]

1 School of Geosciences, China University of Petroleum, Qingdao 266580, China
2 Laboratory for Marine Mineral Resources, Qingdao National Laboratory for Marine Science and Technology, Qingdao 266071, China
3 Key Laboratory of Tectonics and Petroleum Resources (China University of Geosciences), Ministry of Education, Wuhan 430074, China
4 Xinjiang Oilfield Company, PetroChina, Karamay 834000, China

Abstract The Daerbute fault zone, located in the northwestern margin of the Junggar basin, in the Central Asian Orogenic Belt, is a regional strike-slip fault with a length of ~ 400 km. The NE-SW trending Daerbute fault zone presents a distinct linear trend in plain view, cutting through both the Zair Mountain and the Hala'alate Mountain. Because of the intense contraction and shearing, the rocks within the fault zone experienced high degree of cataclasis, schistosity, and mylonization, resulting in rocks that are easily eroded to form a valley with a width of 300–500 m and a depth of 50–100 m after weathering and erosion. The well-exposed outcrops along the Daerbute fault zone present sub-horizontal striations and sub-vertical fault steps, indicating sub-horizontal shearing along the observed fault planes. Flower structures and horizontal drag folds are also observed in both the well-exposed outcrops and high-resolution satellite images. The distribution of accommodating strike-slip splay faults, e.g., the 973-pluton fault and the Great Jurassic Trough fault, are in accordance with the Riedel model of simple shear. The seismic and time-frequency electromagnetic (TFEM) sections also demonstrate the typical strike-slip characteristics of the Daerbute fault zone. Based on detailed field observations of well-exposed outcrops and seismic sections, the Daerbute fault can be subdivided into two segments: the western segment presents multiple fault cores and damage zones, whereas the eastern segment only presents a single fault core, in which the rocks experienced a higher degree of rock cataclasis, schistosity, and mylonization. In the central overlapping portion between the two segments, the sediments within the fault zone are primarily reddish sandstones, conglomerates, and some mudstones, of which the palynological tests suggest middle Permian as the timing of deposition. The deformation timing of the Daerbute fault was estimated by integrating the depocenters' basinward migration and initiation of the splay faults (e.g., the Great Jurassic Trough fault and the 973-pluton fault). These results indicate that there were probably two periods of faulting deformation for the Daerbute fault. By integrating our study with previous studies, we speculate that the Daerbute fault experienced a two-phase strike-slip faulting deformation, commencing with the initial dextral strike-slip faulting in mid-late Permian, and then being inversed to sinistral strike-slip faulting since the Triassic. The results of this study can provide useful insights for the regional tectonics and local hydrocarbon exploration.

Keywords Daerbute fault, structural characteristics, deformation timing, West Junggar

1 Introduction

The Daerbute fault, extending more than 400 km in the NE-SW direction, is the largest and longest-lasting fault structure in the western Junggar area, which exerts an important control on the deformation of the Central Asian orogenic belt (Allen and Vincent, 1997; Zhao et al., 1997; Chen et al., 2010, 2014, 2016; Fan et al., 2014; Yin et al., 2015), the tectonic evolution of the western Junggar region (Zhang et al., 1989; Wu et al., 2013), and related petroleum distribution (Kuang et al., 2008; Shao et al., 2011).

Received February 25, 2017; accepted October 30, 2017

E-mails: Kongyou WU (wukongyou@163.com), Yangwen PEI (peiyangwen@upc.edu.cn)

Previous studies mostly concentrated on the distribution of ophiolites and solid mineral resources along the Daerbute fault zone (e.g., Gu et al., 2009, 2011; Liu et al., 2009; Chen and Guo, 2010; Chen et al., 2011, 2013, 2014, 2015, 2016; Li et al., 2012; Yang et al., 2013b). However, there is still controversy about the fault zone characteristics and fault deformation timing. For the fault properties, Wu (1985) suggested that the Daerbute fault is a tail-extension fault resulted from gravity sliding of the Ke-Xia thrust nappes; other studies believed that the Daerbute fault was a basement-involved thrust-imbrication system (e.g., He et al., 2004, 2006). By integrating the latest geologic evidence, geologists began to identify the strike-slip features of the Daerbute fault (Feng et al., 1990; Allen and Vincent, 1997; Meng et al., 2009; Shao et al., 2011; Fan et al., 2014). In regard to the deformation timing, some research has suggested that the Daerbute fault began faulting deformation in the Carboniferous (Xie et al., 1984; Zhang et al., 1989; Feng et al., 1990), some geologists believed the Daerbute fault was developed in the Permian-Triassic (Sengör et al., 1993; Allen and Vincent, 1997), whereas other studies believed that the Daerbute fault was formed in the Cenozoic (Meng et al., 2009; Yang et al., 2011). By integrating detailed fieldwork data, geophysical data, and palynological data, this study investigated the structural features, characteristics, and kinematic evolution of the Daerbute fault. It is proposed that the Daerbute fault had experienced at least two phases of strike-slip faulting deformation resulting in a tectonic inversion from the initial dextral strike-slip faulting to the later sinistral strike-slip faulting. The Keramay-Baikouquan and Wuerhe-Xiazijie thrust fault zones were involved in the initial dextral strike-slip faulting, and formed flower structures in section view. The results of this study can provide insights on the kinematic evolution of the Daerbute fault, which may help understand regional hydrocarbon migration and accumulation. The field-based observations of fault zones are also important for understanding the fault zone properties, fault zone characteristics, and deformation mechanisms of the northwest Junggar basin.

2 Geologic setting

The Central Asian Orogenic Belt is one of the largest Phanerozoic orogenic belts in the world and has attracted the attention of geologists and geochemists (e.g., Sengör et al., 1993; Xiao et al., 2003; Windley et al., 2007; Jian et al., 2008; Simonov et al., 2015; Tang et al., 2015; Cai et al., 2016). The Central Asian Orogenic Belt extends from the Urals in the west through Kazakhstan, northern China, Mongolia, and southern Siberia to the Okhotsk Sea along the eastern Russian coast (Tang et al., 2012). Previous studies suggested that the Central Asian Orogenic Belt is an accretionary orogenic belt comprised of an accretionary wedge, micro-continental block, trench-arc system, sedimentary basin, and multiple types of igneous rocks (e.g., Xiao et al., 2003; Jian et al., 2008). The kinematic evolution of the Central Asian Orogenic Belt has been divided into three stages: continental margin accretion, post-collision, and intracontinental orogeny (Khain et al., 2002). Regional-scale faults were developed during the orogenesis due to contraction and accretion (Fig. 1). As shown in Fig. 1(a), the western Junggar Orogen, located in the southern Central Asian Orogenic Belt, forms a series of regional-scale strike-slip faults, such as the Baerleike fault, the Toli fault, and the Daerbute fault.

In the western Junggar Orogen, there are three major faulting deformation belts: the Daerbute and Baijiantan ophiolitic belts (e.g., Yang et al., 2012, 2013a; Chen et al., 2014, 2016; Tang et al., 2015), the Daerbute fault zone (e.g., Chen et al., 2014; Yin et al., 2015), and the Karamay-Baikouquan & Wuerhe-Xiazijie fault zones (e.g., Shao et al., 2011; Wu et al., 2014). The Daerbute fault, cutting across the western Junggar orogenic belts, is closely adjacent to the northwestern margin of the oil/gas bearing Junggar basin. Its deformation, together with the Karamay-Baikouquan fault zones and the Wuerhe-Xiazijie fault zones, dominated the interaction between the Junggar basin and orogenic belts to the northwest (Shao et al., 2011). The stratigraphy near the Daerbute fault was dominated by Carboniferous rocks, including eruptive rocks, metamorphic rocks, and minor sedimentary rocks such as sandstones, conglomerates, and mudstones (e.g., Gu et al., 2009, 2011; Liu et al., 2009; Chen and Guo, 2010; Chen et al., 2011, 2013, 2014, 2015, 2016; Li et al., 2012; Yang et al., 2013b). Some locally deposited red conglomerates were observed along the Daerbute fault zone (see the brown shade near the Liushugou profile, in Fig. 1(b)). However, there is still controversy on the timing of the sandy conglomerates. Zhou (1987) suggested that the sandy conglomerates were the early Permian Chidi Formation (P_1ch) according to regional stratigraphic correlation, whereas Allen and Vincent (1997) believed that they should be mid-Permian sediments. Intensive granite intrusions were also developed along the Daerbute fault zone, with ages of 327–271 Ma (Han et al., 2006). An ophiolite belt is also distributed along the Daerbute fault zone with an age of 394.1±6.8 Ma (Gu et al., 2009). Some granite intrusions cut through the Ophiolite belt, resulting in a typical “nailed rock mass” (Han et al., 2010). Widespread stream offset in the Daerbute area also suggests that the strike-slip faulting may continue to the present day with a motion rate of 0.03–0.2 mm/yr (Zhao et al., 1997). In addition, the abundant geologic data, including the broadly developed accommodation faults (Wu et al., 2014) and the locally deposited Permian sediments (Zhou, 1987), provides effective evidence for understanding the kinematic evolution and dynamics of the Daerbute fault (Fig. 1(b)).

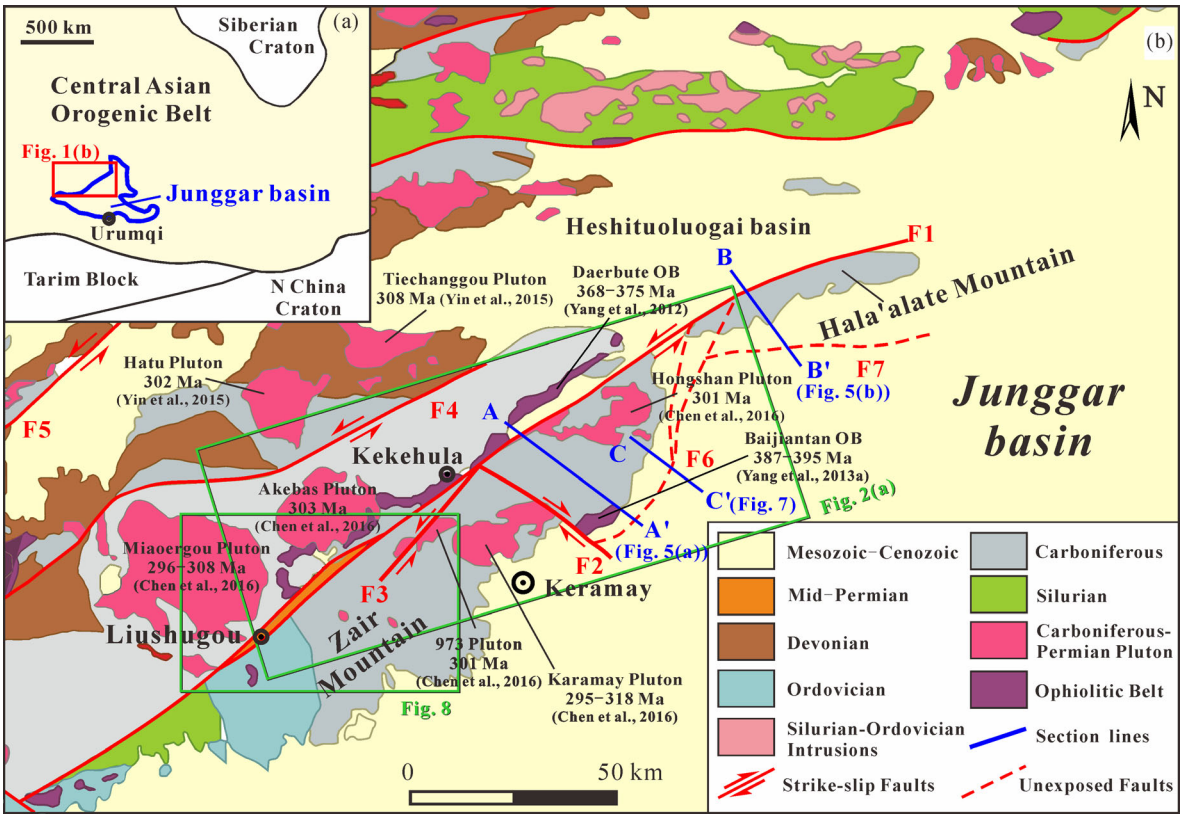

Fig. 1 Geologic setting of the NW Junggar Orogen belt, in which the Daerbute fault zone is an important strike-slip fault in the Central Asian Orogenic Belt. (a) Inset map of the study area in the Central Asian Orogenic Belt. (b) Structural map of the NW Junggar Orogen belt. The Daerbute fault, NE-striking, is a sinistral strike-slip fault that controls the deformation of the Junggar basin. (F1: Daerbute fault; F2: Great Jurassic Trough fault; F3: 973-pluton strike-slip fault; F4: Tuoli fault; F5: Baerleike fault; F6: Karamay-Baikouquan fault; F7: Wuerhe-Xiazijie fault). The U-Pb ages of the intrusions are from Yang et al. (2012, 2013a),Yin et al. (2015), and Chen et al. (2016).

3 Methods

In order to characterize the structural features of the Daerbute strike-slip faulting deformation, we utilized multiple sources of geologic data in this study, including *in-situ* outcrop maps, satellite images, seismic reflection data, time-frequency electromagnetic (TFEM) data, and sporopollen assemblage results. By analyzing these data, we investigated the structural characteristics of the Daerbute fault and its deformation timing and tectonic evolution.

1) Satellite mapping: By integrating field observations, the high-resolution satellite images (from the Google Earth) were interpreted and mapped (Fig. 2) to present the drainage systems, distribution of plutons, and fault systems in the northwestern Junggar area. In particular, the plain view distribution of the Daerbute fault (i.e., F1) and its accommodation splay faults (i.e., F2, the Great Jurassic Trough fault; F3, the 973-pluton fault) were investigated to reveal the tectonic relationship between these strike-slip faults.

2) Detailed outcrop mapping: Well-exposed outcrops of both the Daerbute fault zone and its splay faults were selected for detailed field mapping based on observed structural features in the outcrops (Figs. 3–4), e.g., the Liushugou profile, the Kekehula profile, and the Baiyanghe profile. The outcrops sites, lithology, fault dip/azimuth, and slickensides dip/azimuth were analyzed, which were subsequently used for the kinematic analyses of the Daerbute fault zone.

3) Seismic and time-frequency electromagnetic (TFEM) interpretation: Representative seismic sections (i.e., A-A′ and C-C′) and a time-frequency electromagnetic (TFEM) section (i.e., B-B′) were integrated in this research to understand the subsurface fault architecture of the Daerbute fault zone (Figs. 5–7). The seismic sections in Fig. 5(a) and Fig. 7 are depth-converted and borehole-constrained.

4) Palynology of sedimentary rocks: The sporopollen tests were conducted by the Institute of Experiment and Detection, Xinjiang Oilfield, PetroChina. The results from sporopollen tests of the samples of the fault-bounded sedimentary rocks in the Liushugou profile were used to date the sediments, which was subsequently used to

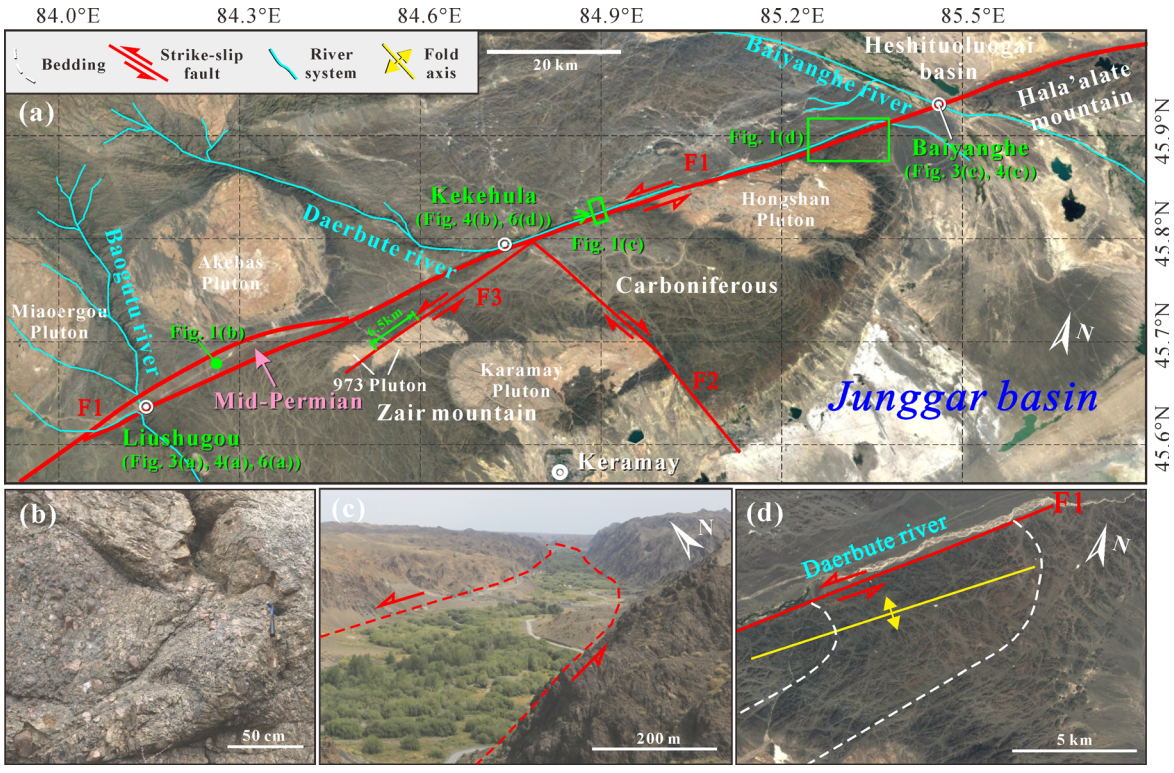

Fig. 2 Satellite image interpretation and structural features of the representative outcrops of the Daerbute fault zone. (a) Satellite image interpretation, including fault trace mapping, river systems, and intrusive plutons. (b) Representative outcrop of the mid-Permian sediments (i.e., sandy conglomerates) that are bounded by the Daerbute fault zone. (c) An overview section from the Kekehula profile, presenting topographic response to the strike-slip faulting of the Daerbute fault. (d) Plain view drag folds developed due to the sinistral strike-slip faulting along the Daerbute fault. F1: Daerbute fault; F2: Great Jurassic Trough fault; F3: 973-pluton fault.

constrain the timing of tectonic inversion between the two-phases of strike-slip faulting deformation in the west Junggar area.

4 Structural characteristics of the Daerbute fault

4.1 Surface fault architecture: outcrops

The rocks in the hanging wall and footwall were entrained in the fault zone and experienced intensive deformation to form anastomosing networks of fractures or faults (Antonellini and Aydin, 1994). According to the degree of fragmentation, a fault zone can be characterized as the central fault core and its adjacent damage zones (Knipe, 1997; Wu et al., 2010; Pei et al., 2015). The NE-SW-trending Daerbute fault presents a linear surface exposure, cutting through the Zair Mountain and the Hala'alate Mountain in the northwest Junggar basin (Fig. 2(a)). The multi-phase tectonic deformation of the Daerbute fault (Allen and Vincent, 1997; Fan et al., 2014) resulted in intensive compression and shearing within the fault core that is therefore easy to be eroded. Under the erosion and transportation by the Daerbute River and other river systems, the present Daerbute fault, extending for hundreds of kilometers, shows as a topographic trough with a width of 300–500 m and a depth of 50–100 m. The topographic trough is filled by the Quaternary sediments transported by the river, and the Carboniferous rocks on both sides of the Daerbute fault are deformed to form the damage zones of the Daerbute fault (Fig. 2(b)).

Based on detailed fieldwork along the Daerbute fault zone, evidence was found to reveal the structural characteristics of the strike-slip faulting deformation of the Daerbute fault.

1) Flower structures: positive flower structures were interpreted in several well-exposed outcrops (Fig. 3). Two well-exposed outcrops that characterize the fault zone architecture are the Liushugou profile (Figs. 3(a) and 3(b)) and the Baiyanghe profile (Figs. 3(c) and 3(d)). The Liushugou profile (Figs. 3(a) and 3(b)) is a SE-striking section that presents the classic geometry of a positive flower structure, with steep primary fault planes and sub-symmetric splay fault planes in the two sides. The rocks experienced strong cataclasis adjacent to the fault slip surfaces whereas the rocks in between the fault surfaces present less strain. Similarly, the Baiyanghe profile (Figs. 3(c) and 3(d)) shows classic positive flower structures that are comprising of central high-angle faults

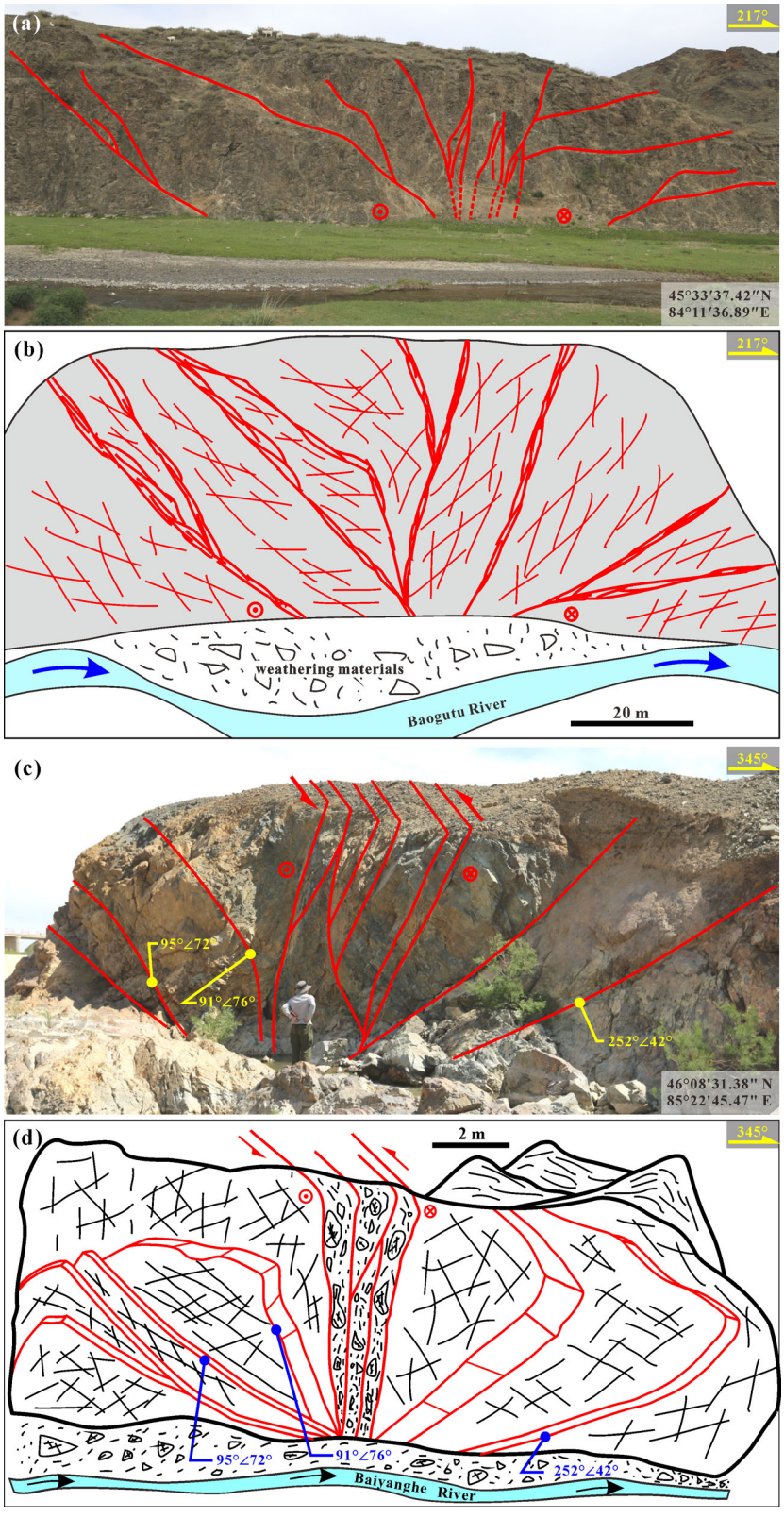

Fig. 3 Interpreted flower structures in well-exposed outcrops and structural sketches at: (a–b) Liushugou profile and (c–d) Baiyanghe profile (see positions of outcrops in Fig. 2(a)). Both profiles present classic positive flower structures, comprising central sub-vertical faults and relatively low-angle splay faults in the two sides.

and relatively low-angle splay faults in the two side walls. In both the two profiles, ~ 80% of the splay faults are broadly cemented by calcite veins, which significantly decreases the porosity and permeability of the rocks to form effective barriers for fluid flows (e.g., Pei et al., 2015).

2) Horizontal slickensides: slickensides are extensively developed in the outcrops in several field sites observed near the Daerbute fault zone, such as the Liushugou profile, the Kekehula profile, and the Baiyanghe profile. Fault steps and slickenfibres are also broadly observed in the fault planes. The slickensides, fault steps, and slickenfibres observed in fault outcrops suggest that the direction of faulting movement is sub-horizontal, with dips ranging from 0°–20° (Fig. 4).

3) Drag folds: in the satellite images, the Carboniferous sediments (in grey color) adjacent to the Daerbute fault present anti-clockwise bending (Fig. 2(d)), of which the fold axis is approximately striking 70°NE. The geometry of drag folds suggests a SW-directing movement of the northwest block of the Daerbute fault, indicating that the present Daerbute fault shows sinistral strike-slip faulting deformation.

4) Strike-slip splay faults: several strike-slip faults developed adjacent to the Daerbute fault zone. The Great Jurassic Trough fault (F2) and the 973-pluton strike-slip fault (F3) are at an acute angle and an approximate right angle to the Daerbute fault, respectively. The 973-pluton was faulted with a sinistral horizontal throw of 6.5 km that is estimated based on satellite image interpretation (Fig. 2 (a)). The Great Jurassic Trough fault is SE-striking and has an almost perpendicular intersection with the Daerbute fault. The Great Jurassic Trough fault offsets the Zair Mountain by ~20 km. The direction of the fault offset suggests dextral strike-slip of the Great Jurassic Trough fault (Wu et al., 2014). These strike-slip faults are synchronously developed together with the Daerbute fault and they obviously have kinematic relationships.

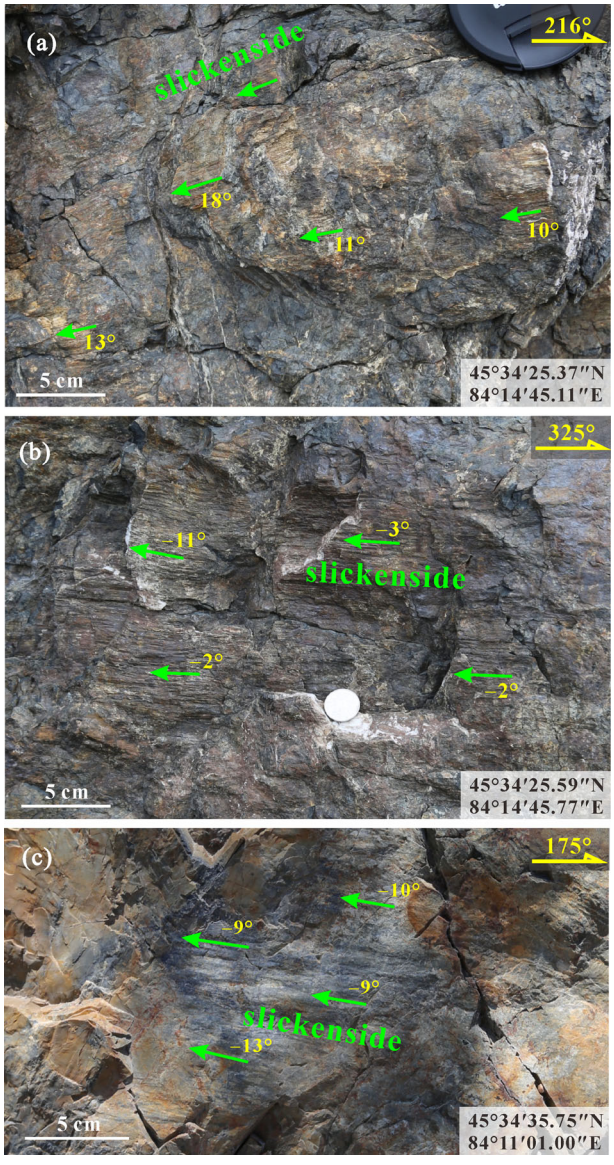

Fig. 4 Horizontal/sub-horizontal slickensides of the outcrops in primary fault plane of the Daerbute fault zone, at the (a) Liushugou profile; (b) Kekehula profile; (c) Baiyanghe profile (see positions of outcrops in Fig. 2(a)). The slickensides present low-angle dips, ranging from 0° to 20°, indicating sub-horizontal shearing between the two walls. The slickensides in these three outcrops all suggest sinistral strike-slip along the fault planes.

4.2 Subsurface fault architecture: seismic and TFEM sections

The subsurface structural characteristics of the Daerbute fault are interpreted by using the latest 2D seismic sections and time-frequency electromagnetic profiles (TFEM) that cross the Zair Mountain (Fig. 5). As shown in Fig. 5(a), positive flower structures are interpreted in the seismic section, indicating the strike-slip features of the Daerbute fault. In the seismic section, the primary fault plane is nearly vertical and cuts down to the basement. On both sides of the primary fault plane, several high-angle reverse faults are developed as the branches of the flower structure. These branches gradually converge to the primary fault plane with increasing depth, forming a typical flower structures in the Daerbute fault zone. However, the flower structure of the Daerbute fault is not symmetric in section view. More branches exist in the southeast side that approaches the adjacent Junggar basin. In the time-frequency electromagnetic profile (TFEM) (Fig. 5(b)), the Daerbute fault also presents well-constrained flower structures, with a primary fault plane vertically cutting into the basement and multiple reverse faults on both sides to form the branches of a flower structure. In this time-frequency electromagnetic profile (TFEM), similar to the seismic section in Fig. 5(a), the flower structure also presents asymmetry with more branch reverse faults on the southeast side adjacent to the Junggar basin. The time-

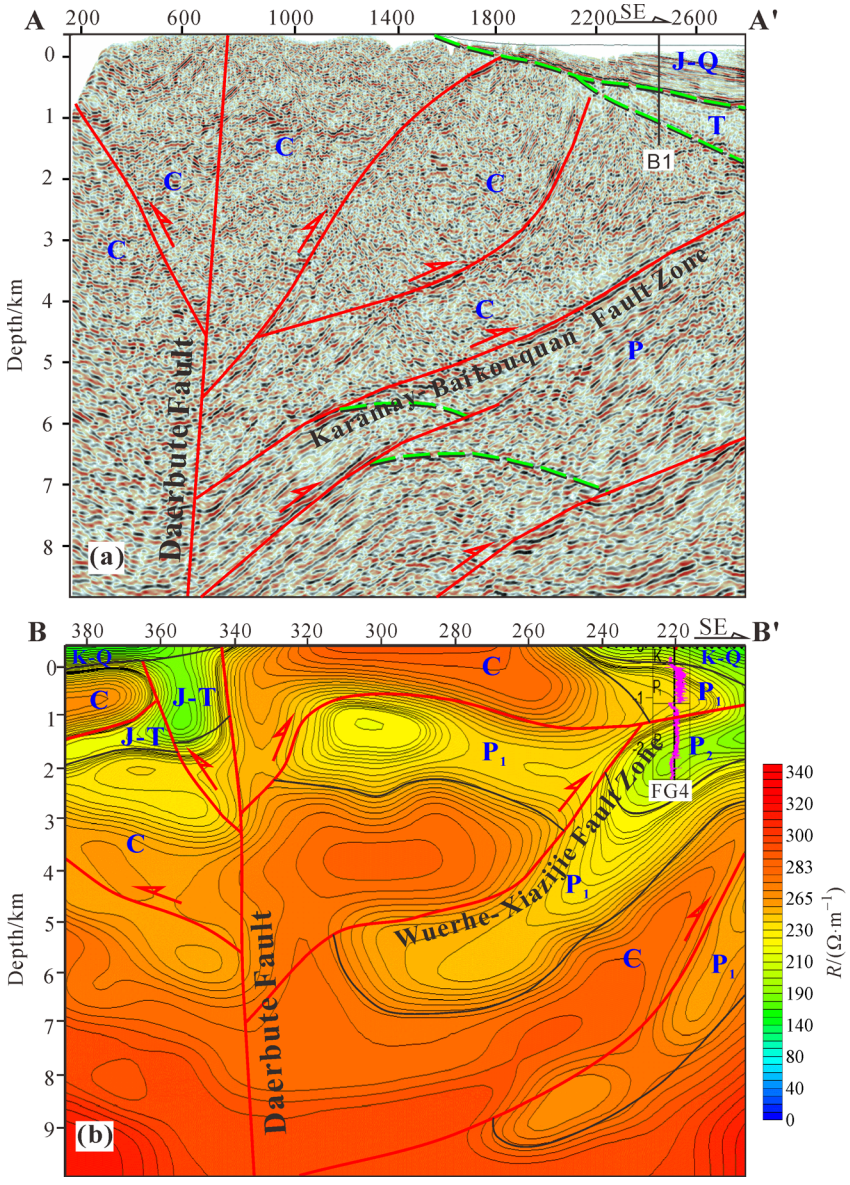

Fig. 5 Interpretation of the seismic reflection and time-frequency electromagnetic sections (TFEM). (a) Seismic section (section A-A′ in Fig. 1); (b) Time-frequency electromagnetic section (TFEM) (section B-B′ in Fig. 1). Based on the seismic reflectors' features, positive flower structures are interpreted, which accounts for the uplift of the Zair Mountain. The time-frequency electromagnetic section (TFEM) also demonstrates structural features that are properly interpreted with positive flower structures. Abbreviations of sediments: C-Carboniferous; P-Permian; P_1-Early Permian; P_2-Middle Permian; T-Triassic; J-Jurassic; K-Cretaceous; Q-Quaternary.

frequency electromagnetic profile (TFEM) reflects a high-gradient of electrical resistivity change, indicating juxtaposition between Paleozoic rocks in hanging walls and Mesozoic sediments in footwalls.

4.3 Segmentation of the Daerbute fault

The Daerbute fault extends more than 400 km in plain view, cutting across the Zair Mountain and the Hala'alate Mountain and forming the boundary between the Junggar basin and the Heshituoluogai basin (Fig. 1). Along its strike, the Daerbute fault is a linear topographic valley with a width of 300–500 m. The Daerbute fault reaches its maximum width at the Liushugou profile (with a width of ~1 km), which is filled by the reddish-brown Permian sandy conglomerates (Figs. 2(a) and 2(b)). The Permian sediments are in direct contact with the Carboniferous rocks in the Daerbute fault zone. Based on field outcrop observations (Fig. 6), the Liushugou profile is a dividing point for the characteristics of the Daerbute fault. To the southwest of the Liushugou profile, the rocks in the fault zone experienced moderate cataclasis and formed multiple fault cores of tens of meters width and multiple damage zones (Figs. 6(a)–6(c)). To the northeast of the Liushugou

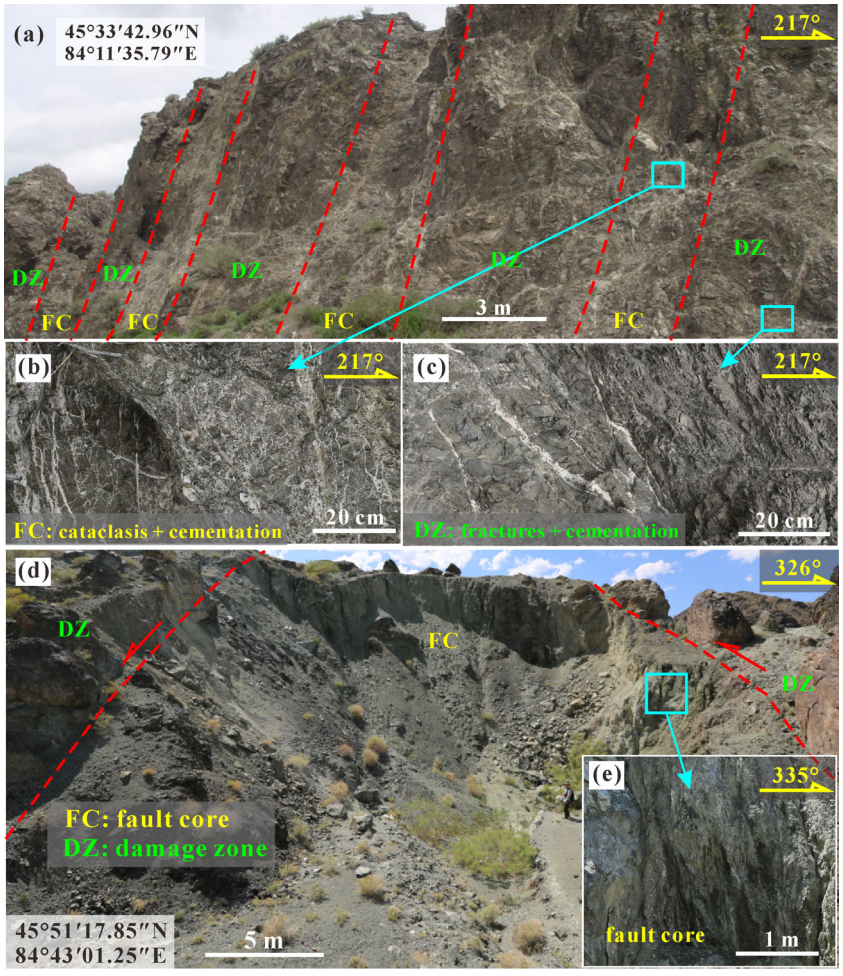

Fig. 6 Structural characteristics of fault zone of the Daerbute fault. (a) Outcrop of eastern segment of the Daerbute fault; (b) outcrop of western segment of the Daerbute fault (see outcrop positions in Fig. 2(a)). Fault cores and damage zones can be interpreted in the representative outcrops based on the magnitude of cataclasis, schistosity and mylonization. FC: fault core; DZ: damage zone.

profile (e.g., the Kekehula area, Figs. 2(c), 6(d)–6(e)), the Carboniferous rocks experienced strong cataclasis to form a single central fault core of hundreds of meters width (Fig. 6(d)). Apparently, the more distributed strain in the southwest portion lead to a higher level of topographic erosion compared to the northeast portion. Correspondingly, the Daerbute fault presents as a wide and open valley in the southwest but a narrow and deep valley in the northeast.

5 Discussion: kinematics of the Daerbute fault

5.1 Deformation timing of the Daerbute fault

The deformation mechanism and deformation timing of the Daerbute fault has been an area of interest for the northwest Junggar basin. Figure 7 presents a high-resolution depth-converted seismic section well constrained by the boreholes GU55, KE98, GU92a, GU53, and 423. In this section, the Karamay-Baikouquan fault zone is upward-steepening towards the Junggar basin, which presents a trishear fault-propagation geometry (e.g., Erslev, 1991; Pei et al., 2014, 2017a, b). The Permian, Triassic, Jurassic, and Cretaceous-Quaternary sediments demonstrate uneven thicknesses from the Karamay-Baikouquan fault zone towards the Junggar basin, suggesting a complex stratigraphic response to the multi-phased faulting deformation. Based on the comparison of the sediments' thickness between the hanging wall and footwall, the Daerbute fault controls the sedimentation of the Permian and younger sediments (Fig. 7), which is in accordance with the results from Zhang and Guo (2010). Published dating results of magmatic rocks in the northwest margin of the Junggar Basin suggested timing of magmatic activities from 340 Ma to 275 Ma, with maximum activity during 310–295 Ma, indicating that plate collision happened during late Carboniferous to early Permian (e.g., Han et al., 2006). In the 2D seismic section going through wells GU55-KE98-

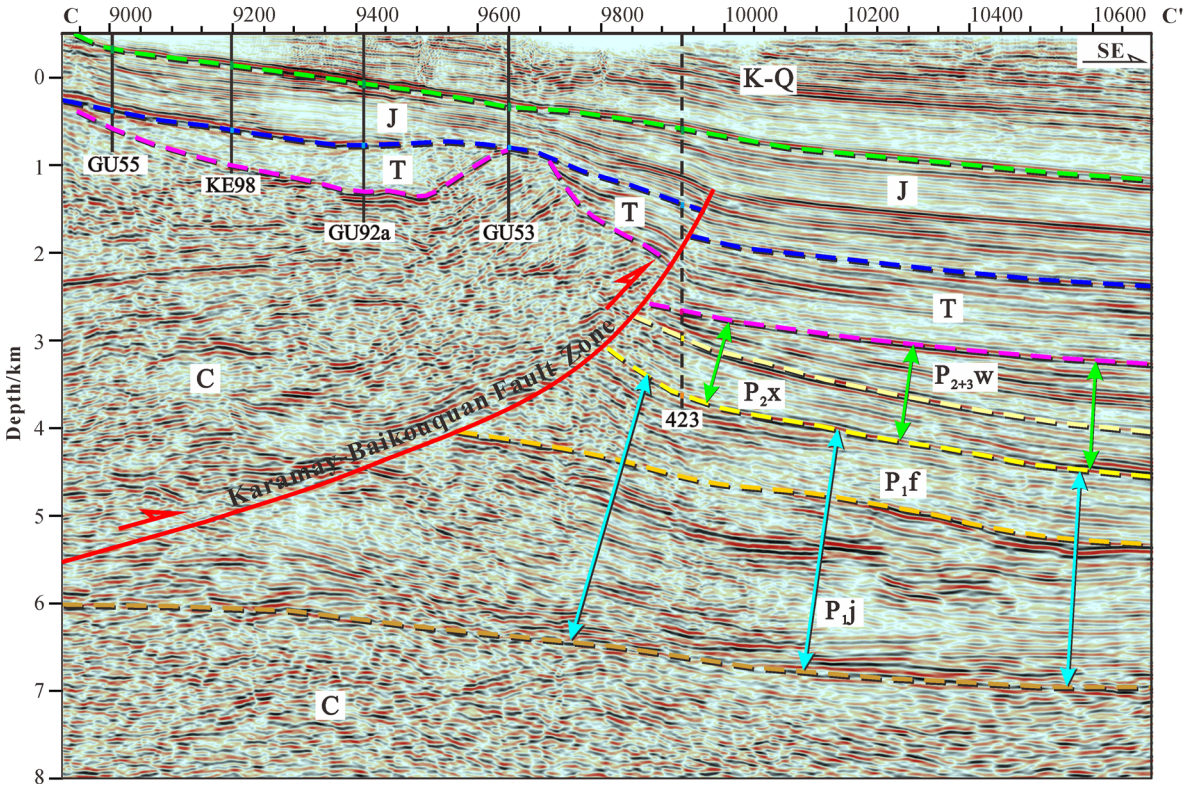

Fig. 7 Seismic interpretation delineating the control of the splay fault (i.e., the Karamay-Baikouquan Fault) of the Daerbute fault on the sedimentation of the northwest Junggar basin. The seismic interpretation of the hanging wall is well-constrained by the wells GU55, KE98, GU92a, and GU53, and the footwall is constrained by well 423 (See position in Fig. 1, section C-C′). Abbreviations of sediments: P_1j-Jiamuhe Formation; P_1f-Fengcheng Formation; P_2x-Xiazijie Formation; $P_{2+3}w$-Wurhe Formation.

GU92a-GU53-423 (Fig. 7), the lower Permian Jiamuhe Formation (P_1j) and Fengcheng Formation (P_1f) present increasing thicknesses when approaching the Daerbute fault, whereas the middle and upper Permian sediments (P_2x and $P_{2+3}w$) present increasing thicknesses towards the Junggar basin. The variation in sediment thickness indicates that a major tectonic event modified the geological settings of the Junggar basin, resulting in the southeast migration of the depocenter from the northwest margin to the internal Junggar basin. This suggests there could be a SE-directing thrusting deformation in the early Permian. In addition, in both outcrops and seismic sections (Figs. 3 and 5), the flower structures present asymmetric geometries. Sui (2015) suggested that the asymmetry of the flower structures along the Daerbute fault zone was probably caused by the superimposition of the later strike-slip faulting since the mid-Permian upon the earlier SE-directing thrusting in late Carboniferous to early Permian. The earlier SE-directing thrusting resulted in multiple low-angle thrust faults towards the Junggar basin, such as the Karamay-Baikouquan fault (F6 in Fig. 1(b)) and Wuerhe-Xiazijie fault (F7 in Fig. 1(b)). Therefore, during the following superimposed strike-slip faulting deformation of the Daerbute fault, the flower structure presents more branch faults towards the Junggar basin. This is in accordance with the previous studies (e.g., Han et al., 2006; Geng et al., 2009; Chen and Guo, 2010; Zhang et al., 2011; Chen et al., 2014, 2016), which described two stages of deformation: 1) the early development of the Daerbute Ophiolitic Belt and the Baijiantan Ophiolitic Belt due to the late Carboniferous and early Permian crustal-scale compression within an remnant ocean basin, and 2) the following sinistral strike-slip faulting deformation due to the far-field effect of the India-Asia collision.

Allen et al. (1995) suggested that there was also a dextral strike-slip component along the Daerbute fault in the first stage. Zhao et al. (1997) observed widespread stream offset in the Daerbute area, suggesting the later sinistral strike-slip faulting may continue to present with a motion rate of 0.03–0.2mm/yr. Due to the strong superimposition of the later sinistral strike-slip faulting deformation (e.g., Wu et al., 2005, 2014), it is difficult to find any direct evidence to validate the initial dextral strike-slip faulting component. However, there are still some lines of indirect evidence that imply the deformation timing of the initial dextral strike-slip faulting component. Based on outcrop observations of the Liushugou profile, younger reddish-brown sandy conglomerates present a linear distribution along the Daerbute fault (Fig. 2(a)). They are poorly rounded and sorted, with an average size up to 20 cm and were derived from the Carboniferous igneous rocks (see Fig. 2(b)). Allen and Vincent (1997) suggested that the deposition of

these conglomerates should be accounted for by the initial dextral strike-slip faulting. However, there is still controversy on the timing of these sandy conglomerates. Zhou (1987) suggested that the sandy conglomerates are the early Permian Chidi Formation (P_1ch) according to regional stratigraphic correlation, whereas Allen and Vincent (1997) believed that it should be the middle Permian sediments. In order to reveal timing of the sandy conglomerates, we collected three samples of the muddy layers interbedded within the sandy conglomerates. Sporopollen fossils in the muddy layers were analyzed with help from the Institute of Experiment and Detection, Xinjiang Oilfield, PetroChina. The sporopollen fossils were dominated by gymnosperm sporopollen (containing Protohaploxypinus and Cordaitina), and characterized by monocolpate sporopollen (Table 1). The Institute of Experiment and Detection (Xinjiang Oilfield, PetroChina) suggested that the characteristics of sporopollen assemblage were similar to that of the middle Permian Wuerhe Formation (P_2w). Therefore, it is inferred that the Daerbute fault presented a dextral strike-slip faulting component in middle Permian and controlled the deposition of the Permian sandy conglomerates. The palynological results are in good agreement with the previous studies, which suggested that the Daerbute fault used to be a dextral strike-slip fault during middle to late Permian (e.g., Feng et al., 1989; Sengör et al., 1993; Allen and Vincent, 1997; Xu et al, 2008b; Shao et al., 2011).

The Great Jurassic Trough fault, cutting through the northwest margin of the Junggar basin, presents strike-slip properties based on both field observations and some previous studies (e.g., Xu et al., 2008a, b). By integrating outcrop observations, subsurface seismic interpretation, and stratigraphic boundaries' cutoffs, the Great Jurassic Trough fault is a dextral strike-slip fault (i.e., F2, in Fig. 2 (a)). The 973-pluton fault (i.e., F3 in Fig. 1 and Fig. 2(a)) presents sinistral strike-slip faulting features, based on the satellite offset of the 973-pluton. The Great Jurassic Trough fault and the 973-pluton fault present an acute angle and an obtuse angle to the Daerbute fault, respectively. In addition, analysis of fluid-inclusion homogenization temperatures and burial history indicate that the Great Jurassic Trough fault was active from the late Triassic to middle Cretaceous (Wu et al., 2014), which provides proper constraints on the timing of the later sinistral strike-slip of the Daerbute fault.

5.2 Tectonic evolution of the Daerbute fault

A set of schematic maps (Fig. 8) were constructed to illustrate the tectonic evolution along the Daerbute fault zone. During the period from the late Carboniferous to the early Permian, a foreland basin, the Junggar basin, was developed due to the thrusting deformation of the western Junggar orogenic belts (Zhang et al., 1998; Lai et al., 1999; Chen et al., 2002; Wu et al., 2005; He et al., 2006). The Lower Permian Jiamuhe Formation and the Fengcheng Formation were deposited, thickening from the Junggar basin towards the Zair Mountain (Fig. 7). During this period, the western Junggar orogenic belt was subject to the SEE-directing compression (e.g., Allen and Vincent, 1997; Xiao et al., 2010; Wang et al., 2011), resulting in the thrusting dominated deformation together with a component of dextral strike-slip of the Daerbute fault (Fig. 8(a)). Due to the fault plane bending near the Liushugou profile, a narrow pull-apart basin probably developed along the Daerbute fault, in which the middle Permian sandy conglomerates were deposited (Fig. 8(a)). These sediments can be potentially used to constrain the deformation timing of the dextral strike-slip faulting of the Daerbute fault. The depocenter was then migrating towards the Junggar basin, resulting in basin-ward thickening of the middle and upper Permian sediments.

Since late Permian, the stress field in the northwestern Junggar basin has been dominated by SSW-NNE compression (Wang et al., 1999; Chen and Guo, 2010; Xiao et al., 2010; Chen et al., 2014, 2016). The Daerbute fault motion was then inversed from the initial dextral strike-slip (Fig. 8(a)) to the later sinistral strike-slip (Fig. 8(b)). The Permian sandy conglomerates were then strongly compressed due to the tectonic inversion and were uplifted and eroded (Fig. 8(b)). In the Cenozoic, due to the India-

Table 1 Results of sporopollen tests of sedimentary rocks in the Liushugou segment of the Daerbute fault. Lithology, coordinates and sporopollen spectrum are provided for the samples

Sample ID	Sampling Sites (GPS)		Lithology	Sporopollen
	Latitude	Longitude		
GSW001	45°34′35.50″N	84°11′09.99″E	Dark mudstone	Leiotriletes spp., Calamospora spp., Punctatisporites spp., Apiculatisporis spp., Raistrickia spp., Kraeuselisporites spp., Pityosporites spp., Crucisaccites spp., Gardenasporites spp., Protohaploxypinus spp., Deltoidospora spp., Concavisporites spp., Cyclogranisporites spp., Granulatisporites spp., Acanthotriletes spp., Verrucosisporites spp., Lycopodiacidites spp., Asseretospora spp., Densosporites spp., Aratrisporites spp., Alisporites spp., Pinuspollenites spp., Podocarpidites spp., Protoconiferus spp., Psophosphera spp., Cycadopites spp., Chasmatosporites sp., Chordasporites spp.
GSW002	45°34′35.50″ N	84°11′09.99″E	Dark mudstone	
GSW003	45°34′30.36″ N	84°11′11.72″ E	Dark mudstone	

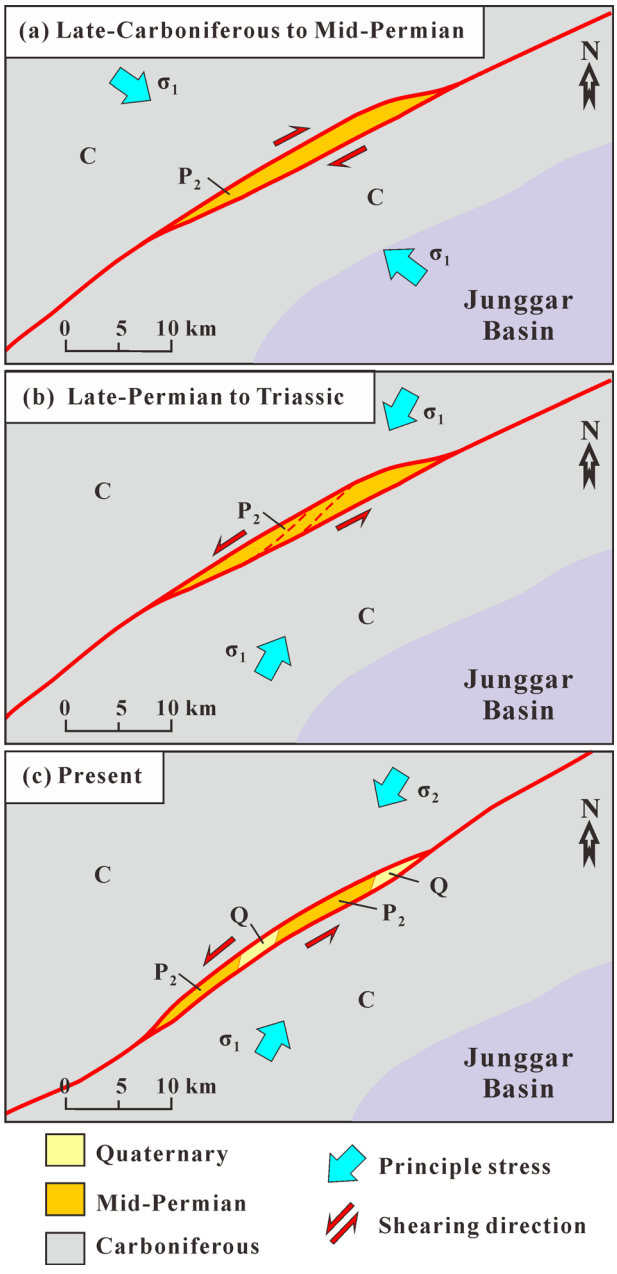

Fig. 8 Schematic maps delineating tectonic evolution of the NW Junggar Orogen belt (see position in Fig. 1 and Fig. 2(a)). The Daerbute fault was initially dextral from the late Carboniferous to the mid-Permian and inversed to be sinistral since the late Permian. This resulted in a pull-apart basin in which the mid-Permian sediments were deposited, being constrained by the splay faults of the Daerbute fault.

Eurasian collision, the west Junggar region was squeezed, and the Daerbute fault remained in sinistral strike-slip faulting under the NNE-SSW compression (Fig. 8(c)).

6 Conclusions

Based on detailed analysis through integrating field outcrop observations, satellite image interpretation, seismic sections, and time-frequency electromagnetic section (TFEM), the following conclusions have been drawn:

1) The Daerbute fault presents a topographic valley with linear distribution, cutting through the Zair and Hala'alate Mountains. The well-exposed outcrops of the Daerbute fault, such as the Liushugou profile, the Kekehula profile, and the Baiyanghe profile, present typical features of strike-slip faulting deformation, e.g., flower structures, horizontal slickensides, plan view drag folds, and strike-slip splay faults. Flower structures interpreted in both seismic sections and time-frequency electromagnetic profiles have validated the structural features observed in the outcrops along the Daerbute fault.

2) The Daerbute fault can be subdivided into northeastern and southwestern segments, based on the field observations. The southwestern segment formed multiple fault cores and damage zones, whereas the northeastern segment formed a single fault core with a larger width. Mylonitization, schistosity, and serpentinization were highly developed in the northeastern segment, due to the high magnitude of shearing and transpression. In the overlapping portion between the northeastern and the southwestern segments, the central fault core, a topographic valley, was filled with middle Permian sandy conglomerates, which could be an indicator of timing of the Daerbute faulting deformation.

3) The Daerbute fault had probably started dextral strike-slip faulting in the middle Permian, forming a small-scale pull-apart mini-basin at a portion of the fault with high curvature, which could allow the deposition of the middle Permian sandy conglomerates. In the Indo Epoch, the Daerbute fault zone was inversed from the initial dextral strike-slip faulting to the later sinistral strike-slip faulting, resulting in the subsequent uplift and erosion of the sandy conglomerates under localized contraction along the Daerbute fault zone.

4) The tectonic evolution of the Daerbute fault played an important control on the stratigraphy and structures in the northwestern margin of the Junggar basin. The initiation of the strike-slip faulting of the Daerbute fault probably indicated the termination of the early foreland basin development, leading to the basin-ward migration of the depocenters. Multiple strike-slip splay faults such as the Great Jurassic Trough fault and the 973-pluton fault were then developed due to the tectonic inversion from the initial dextral strike-slip faulting to the later sinistral strike-slip faulting of the Daerbute fault.

Acknowledgements We would like to thank the Xinjiang Oil Field Company of PetroChina for their permission to use the relevant geological and geophysical data. The constructive comments from the three anonymous reviewers are highly appreciated. This research has been financially supported by: the National Natural Science Foundation of China (Grant Nos. 41272142, 41502192, and 41702138), the National Science and Technology Major Project (2017ZX05001003), Strategic Priority Research Program of Chinese Acdemy of Sciences (XDA14010301), the Provincial

Science Foundation of Shandong Province (No. ZR2012DM011), and the Open Funding of the Key Laboratory of Tectonics and Petroleum Resources (No. TPR-2016-02).

References

Allen M B, Eengor A M C, Natal'In B A (1995). Junggar, Turfan and Alakol basins as Late Permian to Early Triassic extensional structures in a sinistral shear zone in the Altaid orogenic collage, Central Asia. J Geol Soc London, 152(2): 327–338

Allen M B, Vincent S J (1997). Fault reactivation in the Junggar region, northwest China: the role of basement structures during Mesozoic-Cenozoic compression. J Geol Soc London, 154(1): 151–155

Antonellini M, Aydin A (1994). Effect of faulting on fluid flow in porous sandstones: petrophysical properties. AAPG Bull, 78(3): 355–377

Cai K, Sun M, Buslov M M, Jahn B, Xiao W, Long X, Chen H, Wan B, Chen M, Rubanova E S, Kulikova A V, Voytishek E E (2016). Crustal nature and origin of the Russian Altai: implications for the continental evolution and growth of the Central Asian Orogenic Belt (CAOB). Tectonophysics, 674: 182–194

Chen J F, Han B F, Zhang L (2010). Geochemistry, Sr-Nd isotopes and tectonic implications of two generations of Late Paleozoic plutons in northern West Junggar, Northwest China. Acta Petrologica Sinica, 26 (8): 2317–2335 (in Chinese)

Chen S, Guo Z J (2010). Time constraints, tectonic setting of Dalabute ophiolitic complex and its significance for late Paleozoic tectonic evolution in West Junggar. Acta Petrologica Sinica, 26(8): 2336–2344 (in Chinese)

Chen S, Guo Z J, Pe-piper G, Zhu B B (2013). Late Paleozoic peperites in West Junggar, China, and how they constrain regional tectonic and palaeoenvironmental setting. Gondwana Res, 23(2): 666–681

Chen S, Guo Z J, Qi J F, Xing X R (2016). Three-stage strike-slip fault systems at northwestern margin of Junggar Basin and their implications for hydrocarbon exploration. Oil and Gas Geology, 37 (3): 322–331 (in Chinese)

Chen S, Pe-Piper G, Piper D J W, Guo Z J (2014). Ophiolitic mélanges in crustal-scale fault zones: implications for the Late Palaeozoic tectonic evolution in West Junggar, China. Tectonics, 33(12): 2419–2443

Chen X H, Nie L S, Ding W C, Wang X Q, Wang Z H, Ye B Y (2015). The relationship between strike-slip tectonic system and geochemical anomalies in the West Junggar, northwestern China and its implication for mineral exploration. Acta Petrologica Sinica, 31(2): 371–387 (in Chinese)

Chen X H, Yang N, Ye B Y, Wang Z H, Chen Z L (2011). Tectonic system and its control on metallogenesis in western Junggar as part of the central Asia multi-core metallogenic system. Geotectonica et Metallogenia, 2011, 35(3): 325–338 (in Chinese)

Chen X, Lu H X, Shu L S, Wang H M, Zhang G Q (2002). Study on tectonic evolution of Junggar Basin. Geological Journal of China Universities, 8(3): 257–266 (in Chinese)

Erslev E (1991). Trishear fault-propagation folding. Geology, 19(6): 617–620

Fan C, Su Z, Zhou L (2014). Kinematic features of Darlbute fault in northwestern margin of Junggar Basin. Chinese Journal of Geology, 49(4): 1045–1058 (in Chinese)

Feng H R, Li X, Liu J Q (1990). The structural evolution of the Darabut fault system in West Jungger. Journal of Xi'an University of Geosciences, 12(2): 46–55 (in Chinese)

Feng Y M, Coleman R G, Tilton G, Xiao X (1989). Tectonic evolution of the west Jungger region, Xinjiang, China. Tectonics, 8(4): 729–752 (in Chinese)

Geng H Y, Sun M, Yuan C, Xiao W J, Xian W S, Zhao G C, Zhang L F, Wong K, Wu F Y (2009). Geochemical, Sr–Nd and zircon U–Pb–Hf isotopic studies of Late Carboniferous magmatism in the West Junggar, Xinjiang: implications for ridge subduction? Chem Geol, 266(3–4): 364–389

Gu P Y, Li Y J, Wang X G, Zhang H W, Wang J N (2011). Geochemical evidences and tectonic significances of Dalabute SSZ-type ophiolitic melange, Western Junggar Basin. Geological Review, 57(1): 36–43 (in Chinese)

Gu P Y, Li Y J, Zhang B, Tong L L, Wang J N (2009). LA-ICP-MS zircon U-Pb dating of gabbro in the Darbut ophiolite, western Junggar, China. Acta Petrologica Sinica, 25(6): 1364–1372 (in Chinese)

Han B F, Guo Z J, He G Q (2010). Timing of major suture zones in North Xinjiang, China: constraints from stitching plutons. Acta Petrologica Sinica, 26(8): 2233–2246 (in Chinese)

Han B F, Ji J Q, Song B, Chen L H, Zhang L (2006). Late Paleozoic vertical growth of continental crust around the Junggar Basin, Xinjiang, China (Part I): timing of post-collisional plutonism. Acta Petrologica Sinica, 22(5): 1077–1086 (in Chinese)

He D F, Guan S W, Zhang N F, Wu X Z, Zhang Y Q (2006). Thrust Belt structure and significance for petroleum exploration in Hala'alat Mountain in northwestern margin of Junggar Basin. Xinjiang Petroleum Geology, 27(3): 267–269 (in Chinese)

He D F, Yin C, Du S K, Shi X, Ma H S (2004). Characteristics of structural segmentation of foreland thrust belts—A case study of the fault belts in the northwestern margin of Junggar Basin. Earth Sci Front, 11(3): 91–101 (in Chinese)

Jian P, Liu D, Kröner A, Windley B F, Shi Y, Zhang F, Shi G, Miao L, Zhang W, Zhang Q, Zhang L, Ren J (2008). Time scale of an early to mid-Paleozoic orogenic cycle of the long-lived Central Asian Orogenic Belt, Inner Mongolia of China: implications for continental growth. Lithos, 101(3–4): 233–259

Khain E V, Bibikova E V, Kroner A, Zhuravlev D Z, Sklyarov E V, Fedotova A A, Kravchenko-Berezhnoy I R (2002). The most ancient ophiolite of the Central Asian fold belt: U–Pb and Pb–Pb zircon ages for the Dunzhugur Complex, Eastern Sayan, Siberia, and geodynamic implications. Earth Planet Sci Lett, 199(3–4): 311–325

Knipe R J (1997). Juxtaposition and seal diagrams to help analyze fault seals in hydro-carbon reservoirs. AAPG Bulletin, 81 (2): 187–195

Kuang J, Zhang Y Q, Hou L H (2008). Exploratory targets of Karamay-Baikouquan buried structural belt in northwestern margin of Junggar Basin. XinJiang Petroleum Geology, 29(4): 431–434 (in Chinese)

Lai S X, Huang K, Chen J L, Wu J, Qian W C, Chen S P, Xu H M (1999). The foreland basin evolution and hydrocarbon accumulation of Late Carboniferous and Permian of the Junggar Basin. Xinjiang Petroleum Geology, 20(4): 293–297 (in Chinese)

Li Y J, Wang R, Li W D, Tong L L, Zhang B, Yang G X, Wang J N, Zhao Y M (2012). Discovery of the porphyry copper-molybdenum deposits and prospecting reflections in southern Darbut tectonic

magmatic belts, West Junggar, China. Acta Petrologica Sinica, 28(7): 2009–2014 (in Chinese)

Liu X J, Xu J F, Wang S Q, Hou Q Y, Bai Z H, Lei M (2009). Geochemistry and dating of E-MORB type mafic rocks from Dalabute ophiolite in West Junggar, Xinjiang and geological implications. Acta Petrologica Sinica, 25(6): 1373–1389 (in Chinese)

Meng J F, Guo Z J, Fang S H (2009). A new insight into the thrust structures at the northwestern margin if Junggar Basin. Earth Sci Front, 03: 171–180 (in Chinese)

Pei Y, Paton D A, Knipe R J (2014). Defining a 3-dimensional trishear parameter space to understand the temporal evolution of fault propagation folds. J Struct Geol, 66: 284–297

Pei Y, Paton D A, Knipe R J, Wu K (2015). A review of fault sealing behaviour and its evaluation in siliciclastic rocks. Earth Sci Rev, 150: 121–138

Pei Y, Paton D A, Knipe R J, Wu K (2017a). Examining fault architecture and strain distribution using geospatial and geomechanical modelling: an example from the Qaidam basin, NE Tibet. Mar Pet Geol, 84: 1–17

Pei Y, Paton D A, Wu K, Xie L (2017b). Subsurface structural interpretation by applying trishear algorithm: an example from the Lenghu5 fold-and-thrust belt, Qaidam Basin, Northern Tibetan Plateau. J Asian Earth Sci, 143: 343–353

Sengör A M C, Natal'in B A, Burtman V S (1993). Evolution of the Altaid tectonic collage and Palaeozoic crustal growth in Eurasia. Nature, 364(6435): 299–307

Shao Y, Wang R F, Zhang Y Q, Wang X, Li Z H, Liang H (2011). Strike-slip structures and oil-gas exploration in the NW margin of the Junggar Basin, China. Acta Petrol Sin, 32(6): 976–984 (in Chinese)

Simonov V A, Mikolaichuk A V, Safonova I Y, Kotlyarov A V, Kovyazin S V (2015). Late Paleozoic–Cenozoic intra-plate continental basaltic magmatism of the Tienshan–Junggar region in the SW Central Asian Orogenic Belt. Gondwana Res, 27(4): 1646–1666

Sui F G (2015). Tectonic evolution and its relationship with hydrocarbon accumulation in the northwest margin of Junggar Basin. Acta Geol Sin, 89(4): 779–793 (in Chinese)

Tang G J, Wang Q, Wyman D A, Li Z X, Zhao Z H, Yang Y H (2012). Late Carboniferous high ϵNd(t)–ϵHf(t) granitoids, enclaves and dikes in western Junggar, NW China: ridge-subduction-related magmatism and crustal growth. Lithos, 140–141: 86–102

Tang J, He D, Li D, Ma D (2015). Large-scale thrusting at the northern Junggar Basin since Cretaceous and its implications for the rejuvenation of the Central Asian Orogenic Belt. Geoscience Frontiers, 6(2): 227–246

Wang W F, Wang Y, Lu S K (1999). Structural belts and deformation features of the Junggar Basin. Seismology and Geology, 21(4): 324–333 (in Chinese)

Wang Y X, Hou G T, Liu S L, , Li L, Niu X L, Xiao F F (2011). Numerical simulation of tectonic dynamics of the Junggar basin at the end of Paleozoic. Chin J Geophys, 54(2): 441–448 (in Chinese)

Windley B F, Alexeiev D, Xiao W, Kröner A, Badarch G (2007). Tectonic models for accretion of the Central Asian Orogenic Belt. J Geol Soc London, 164(1): 31–47

Wu H E, Chen X W, Yang M Z, Xu D L (2013). Preliminary Exploration on the formation of the Structural grid of the Baogutu Structural Block in the Southeastern of the Darbute of the West Junggar. XinJiang YouSe JinShu, 5: 52–55 (in Chinese)

Wu K Y, Qu J H, Wang H H (2014). Strike-slip characteristics, forming mechanisms and controlling reservoirs of Dazhuluogou fault in Junggar Basin. Journal of China University of Petroleum (Edition of Natural Science), 38(5): 41–47 (in Chinese)

Wu K Y, Zha M, Wang X L, Qu J X, Chen X (2005). Further researches on the tectonic evolution and dynamic setting of the Junggar Basin. Acta Geoscientica Sinica, 26(3): 217–222 (in Chinese)

Wu Q F (1985). On the mechanism of formation of the Klamayi-Xiazijie Nappe. J Petrol, 6(3): 29–34 (in Chinese)

Wu Z P, Chen W, Xue Y, Song G Q, Liu H M (2010). Structural characteristics of faulting zone and its ability in transporting and sealing oil and gas. Acta Geol Sin, 84(4): 570–578 (in Chinese)

Xiao F F, Hou G T, Wang Y X, Li L (2010). Study on structural stress fields since Permian, Junggar Basin and adjacent areas. Acta Scientiarum Naturalium Universitatis Pekenensis, 46(2): 224–230 (in Chinese)

Xiao W, Windley B F, Hao J, Zhai M (2003). Accretion leading to collision and the Permian Solonker suture, Inner Mongolia, China: termination of the central Asian orogenic belt. Tectonics, 22 (6): 8-1–8-20

Xie H, Zhao B, Lin L D, You Q M (1984). Oil characteristics of the overthrusts zone of the northwestern margin of the Junggar Basin. Xinjiang Petroleum Geology, 4(3): 1–15 (in Chinese)

Xu H M, Xu Z H, Li Z H, Liu D G, Chen Y U, Liu W (2008a). Characteristics of strike-slip faults in the northwestern margin of Junggar Basin and their geological significance for petroleum. Geological Journal of China Universities, 14(2): 217–222 (in Chinese)

Xu Z H, Xu H M, Lin J, Peng J C, Zhang B, Zhang G Q (2008b). 256 Strike-slip fault zone characteristic and its geological significance in northwestern margin of Junggar Basin. Xinjiang Petroleum Geology, 29(3): 309–310 (in Chinese)

Yang G X, Li Y J, Gu P Y, Yang B K, Tong L L, Zhang H W (2012). Geochronological and geochemical study of the Darbut Ophiolitic Complex in the West Junggar (NW China): implications for petrogenesis and tectonic evolution. Gondwana Res, 21(4): 1037–1049

Yang G X, Li Y J, Santosh M, Yang B K, Zhang B, Tong L L (2013a). Geochronology and geochemistry of basalts from the Karamay ophiolitic mélange in West Junggar (NW China): implications for Devonian-Carboniferous intra-oceanic accretionary tectonics of the southern Altaids. Geol Soc Am Bull, 125(3–4): 401–419

Yang G X, Li Y J, Yang B K, Liu Z W, Zhang H W, Tong L L (2013b). Petrogenesis of alkaline basalt from the Darbut ophiolitic mélange in West Junggar: the product of a late Devonian mantle plume? Earth Sci Front, 20(3): 192–203 (in Chinese)

Yang G, Wang X B, Li B L, Shi X (2011). Transpression and wrench faults of northwestern margin of Junggar Basin. Chinese Journal of Geology, 46(3): 696–708 (in Chinese)

Yin J Y, Chen W, Xiao W J, Yuan C, Sun M, Tang G J, Yu S, Long X P, Cai K D, Geng H Y, Zhang Y, Liu X Y (2015). Petrogenesis of Early-Permian sanukitoids from West Junggar, Northwest China: implications for Late Paleozoic crustal growth in Central Asia. Tectonophysics, 662: 385–397

Zhang G C, Liu L J, Chen X F, Liu J W (1998). Structure and trap types of Junggar Basin. XinJiang Geology, 16(3): 221–229 (in Chinese)

Zhang J E, Xiao W J, Han C M, Ao S J, Yuan C, Sun M, Geng H Y, Zhao G C, Guo Q Q, Ma C (2011). Kinematics and age constraints of deformation in a Late Carboniferous accretionary complex in Western Junggar, NW China. Gondwana Res, 19(4): 958–974

Zhang Q H, Wei Z L, Sun S H (1989). The formation age of the Darlbute fault zone of the west Junggar Basin. Xinjiang Petroleum Geology, 10(1): 35–38 (in Chinese)

Zhang Y Y, Guo Z J (2010). New constraints on formation ages of ophiolites in northern Junggar and comparative study on their connection. Acta Petrologica Sinica, 26(2): 421–430 (in Chinese)

Zhao R, Li J, Shi S, Yang Z (1997). Structural activity of middle Daerbute fault. Inland Earthquake, 11(4): 295–301 (in Chinese)

Zhou L R (1987). Early Permian strata in the Geosyncline fold belt of the West Junggar Basin. Northwest Geol, 3(2): 20–26